ARTICLE

OBC
www.rsc.org/obc

The role of the disulfide bond in amyloid-like fibrillogenesis in a model peptide system

Apurba Kumar Das,[a] Michael G. B. Drew,[b] Debasish Haldar[a] and Arindam Banerjee*[a]

[a] *Department of Biological Chemistry, Indian Association for the Cultivation of Science, Jadavpur, Kolkata 700 032, India. E-mail: bcab@mahendra.iacs.res.in; Fax: +91-33-2473-2805*

[b] *School of Chemistry, The University of Reading, Whiteknights, Reading, UK RG6 6AD*

Received 28th June 2005, Accepted 20th July 2005
First published as an Advance Article on the web 11th August 2005

Three terminally protected short peptides Bis[Boc–D-Leu(1)–Cys(2)–OMe] **1**, Bis[Boc–Leu(1)–Cys(2)–OMe] **2** and Bis[Boc–Val(1)–Cys(2)–OMe] **3** exhibit amyloid-like fibrillar morphology. Single crystal X-ray diffraction analysis of peptide **1** clearly demonstrates that it adopts an overall extended backbone molecular conformation that self-assembles to form an intermolecular hydrogen-bonded antiparallel supramolecular β-sheet structure in crystals. Scanning electron microscopic (SEM) images, transmission electron microscopic (TEM) images and Congo red binding studies vividly demonstrate the amyloid-like fibril formation of peptides **1**, **2** and **3**. However, after reduction of the disulfide bridge of peptides **1**, **2** and **3**, three newly generated peptides Boc–D-Leu(1)–Cys(2)–OMe **4**, Boc–Leu(1)–Cys(2)–OMe **5** and Boc–Val(1)–Cys(2)–OMe **6** are formed and all of them failed to form any kind of fibril under the same conditions, indicating the important role of the disulfide bond in amyloid-like fibrillogenesis in a peptide model system.

Introduction

Self-assembly of short model peptides containing suitable molecular conformations to form supramolecular β-sheet architecture is a highly emerging field of current research.[1,2] Recent reports have demonstrated that self-assembling β-sheet peptide scaffolds can act as biomaterials for neurite outgrowth and they are useful for tissue repair and tissue engineering.[3] Accumulating evidence indicates that many fatal neurodegenerative diseases including Alzheimer's disease,[4] Huntington's disease,[5] Parkinson's disease[6] and prion related encephalopathies[7] occur due to the formation and deposition of amyloid fibrils as plaques in specific regions of the brain. Other examples of amyloid diseases include type II diabetes where misfolded islet amyloid polypeptides (IAPP) form amyloid fibrils in the pancreas[8] and fatal familial cardiomyopathy amyloid deposition occurs in cardiac tissues.[9] Patients undergoing long term haemo-dialysis generally suffer from β2-microglobulin (β2M) amyloidosis.[10] Recently, Goto and coworkers have established that the disulfide bond plays an essential role in the amyloid fibril formation of β2-microglobulin.[10] A recent report also suggests that in transthyretin amyloidosis, Cys10 mixed disulfides of TTR mutants are more amyloidogenic than the wild type transthyretin under mildly acidic conditions.[11] Austen and his coworkers have demonstrated that a disulfide bond is required for the formation of β-sheet structure and amyloid fibrils in Familial British Dementia (FBD), a rare autosomal dominant neurodegenerative disorder that shares features of Alzheimer's disease.[12]

Previously, Atkins and Lyon have shown that the oxidized disulfide form of glutathione self-assembles into an extended network of intermolecular, antiparallel sheets in appropriate organic solvents to form gels.[13] We are involved in developing model peptides that form supramolecular parallel or antiparallel β-sheets in crystals and amyloid-like fibrils in the solid state[14] and we are interested in investigating the role of the disulfide bond in amyloid-like fibril formation in our model peptide system. To this end we have synthesized three terminally protected short model peptides Bis[Boc–D-Leu(1)–Cys(2)–OMe] **1**, Bis[Boc–Leu(1)–Cys(2)–OMe] **2** and Bis[Boc–Val(1)–Cys(2)–OMe] **3** (Fig. 1). Compounds Boc–D-Leu(1)–Cys(2)–OMe **4**, Boc–Leu(1)–Cys(2)–OMe **5** and Boc–Val(1)–Cys(2)–OMe **6**

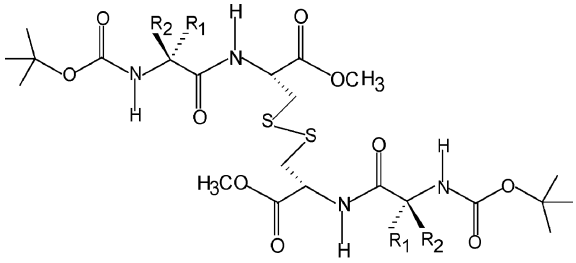

Peptide **1**: $R_1 = CH_2CH(CH_3)_2$, $R_2 = H$
Peptide **2**: $R_1 = H$, $R_2 = CH_2CH(CH_3)_2$
Peptide **3**: $R_1 = H$, $R_2 = CH(CH_3)_2$

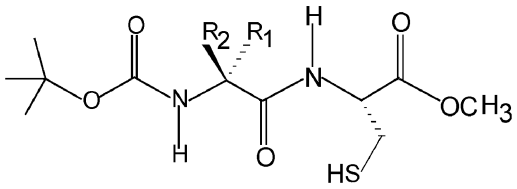

Peptide **4**: $R_1 = CH_2CH(CH_3)_2$, $R_2 = H$
Peptide **5**: $R_1 = H$, $R_2 = CH_2CH(CH_3)_2$
Peptide **6**: $R_1 = H$, $R_2 = CH(CH_3)_2$

Fig. 1 The schematic presentation of peptides **1–6**.

(Fig. 1) were obtained from the reduction of the disulfide bond of peptides **1**, **2** and **3**. In this paper we address the question of whether the presence of the disulfide bridge is necessary to form amyloid-like fibrils or not. We present here the detailed structural analysis of peptide **1** using single crystal X-ray diffraction study and the fibrillation study of this peptide and other structure related peptides (peptides **2** and **3**) in the solid state. Congo red binding studies of the fibrils generated from peptides **1**, **2** and **3** were performed in order to probe whether these fibrils are amyloid-like or not. Whether the peptides with reduced disulfide bonds (peptides **4**, **5** and **6**) can form fibrils is also addressed here.

DOI: 10.1039/b509083k

Results and discussion

Single crystal X-ray diffraction study

Colorless monoclinic crystals of peptide **1**, suitable for an X-ray diffraction study were obtained from a methanol–water solution by slow evaporation. The molecule shown in Fig. 2 contains a crystallographic C2 axis though the S–S bond. There are no intramolecular hydrogen bonds. The dihedral angle values $\phi 1$ (122.2(6)°) and $\psi 1$ (−111.2(5)°) fall within the parallel β-sheet region whereas $\phi 2$ (50.1(6)°) and $\psi 2$ (40.6(6)°) fall within the right handed α-helical region of the Ramachandran map.[15] Here, the adoption of positive ϕ, ψ values of the D-leucine residue is a common feature. However, the molecular conformation of this peptide looks like an overall extended backbone β-strand structure (Fig. 2). There is an intramolecular disulfide bond that connects the two similar parts of the molecule (Fig. 1). The dihedral angle around the S–S bond is 87.9(2)°. Self-assembly of the individual monomers leads to the formation of a β-sheet ribbon along the crystallographic *b* axis (Fig. 3). The β-sheet ribbon structure is stabilized by four intermolecular hydrogen bonds (two from each part of the molecule) N3–H3 · · · O4 and N6–H6 · · · O7 (Table 1) that connect the individual peptide molecules. Each β-sheet column is then stacked *via* van der Waals interactions to form a highly ordered supramolecular structure along the axis parallel to the crystallographic *c* direction (Fig. 4). Fig. 5 presents a schematic illustration of the stepwise self-assembly of peptide **1** into the supramolecular β-sheet architecture.

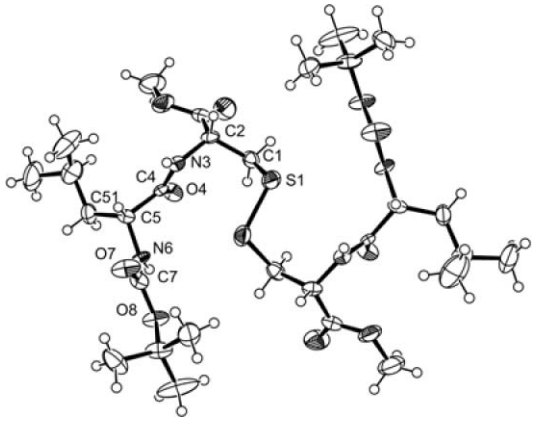

Fig. 2 The ORTEP diagram of peptide **1** with atomic numbering scheme. Ellipsoids are at a level of 30% probability.

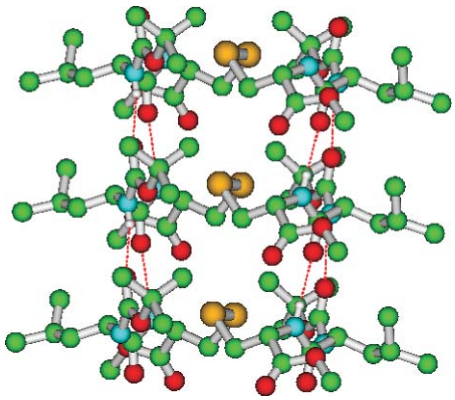

Fig. 3 Packing of peptide **1**, showing the self-assembly of individual monomers, leads to the formation of an intermolecular hydrogen-bonded supramolecular β-sheet ribbon structure along the crystallographic *b* axis. Hydrogen bonds are shown as dotted lines.

Table 1 Intermolecular hydrogen bonding parameters of peptide **1** in the crystal state

D–H · · · A	H · · · A/Å	D · · · A/Å	D–H · · · A/°
N3–H3 · · · O4[a]	2.18	3.04	178
N6–H6 · · · O7[b]	2.13	2.98	169

[a] Symmetry element x, $1 + y$, z. [b] Symmetry element x, $-1 + y$, z.

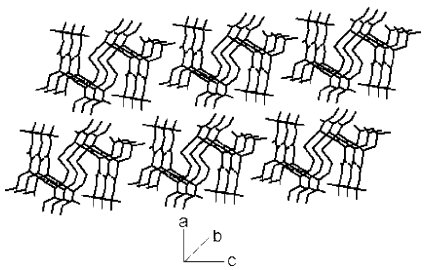

Fig. 4 Higher order packing of peptide **1** along the crystallographic *c* axis forming quaternary β-sheet structures. Hydrogen bonds are shown as dotted lines.

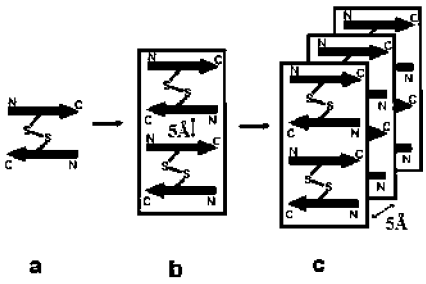

Fig. 5 Schematic illustration of the stepwise self-assembly of disulfide bridge peptide **1** into the supramolecular β-sheet architecture.

FT-IR studies

The FT-IR studies of all reported peptides indicate that NH-stretching vibrations fall within the range from 3315–3341 cm^{-1} corresponding to an intermolecular H-bonded aggregated structure and the CO-stretching vibrations are within the range from 1653–1689 cm^{-1} (Table 2) which are suggestive of intermolecularly H-bonded aggregated sheet-like structures for these peptides in the solid state.[16]

Morphological study

To examine the role of the disulfide bond in fibril formation, morphological studies of peptides **1**, **2** and **3** were carried out using a scanning electron microscope (SEM) and a transmission electron microscope (TEM). The SEM images of peptides **1**, **2** and **3** (Fig. 6) of the dried fibrous material grown from methanol–water clearly demonstrate that the aggregates in the solid state have amyloid-like fibrillar morphology.[17] The SEM image of peptide **1** shows the entangled fibrillar network structure while the SEM image of peptide **2** exhibits the filamentous fibrillar structure. Fig. 6(c) shows the SEM picture

Table 2 Infrared (IR) absorption frequencies (cm^{-1}) for all reported peptides in the solid state (on a KBr pellet)

Peptide	CO stretch	NH bend	NH stretch
1	1655 (s)	1532 (m)	3331 (s)
2	1664 (s)	1540 (m)	3315 (s)
3	1654 (s)	1532 (m)	3330 (s)
4	1662 (s)	1527 (m)	3341 (s)
5	1679 (s)	1540 (m)	3337 (s)
6	1689 (s), 1653 (m)	1531 (m)	3330 (s)

s = strong, m = medium

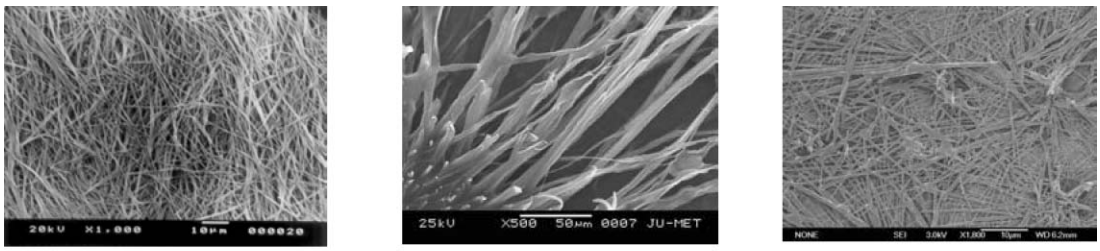

(a) (b) (c)

Fig. 6 SEM images of (a) peptide **1** showing fibrillar morphology, (b) peptide **2** showing filamentous fibrillar morphology and (c) peptide **3** showing fibrillar morphology in the solid state.

of peptide **3** suggesting a fibrillar network structure. The TEM image of peptide **1** also shows remarkable amyloid-like fibrillar morphology (Fig. 7). The representative TEM image of peptide **1** reveals that the peptide exists as a bunch of long unbranched filaments. However, peptides **4**, **5** and **6** have failed to form any kind of fibril under the same conditions. The SEM image of peptide **6** does not show any kind of fibrillar structure in the solid state (Fig. 8).

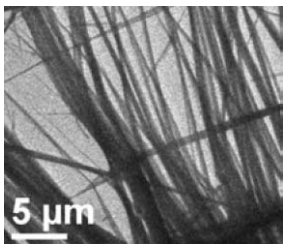

Fig. 7 TEM image of peptide **1** shows amyloid-like fibrillar morphology in the solid state.

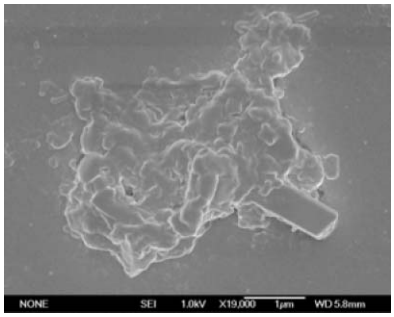

Fig. 8 SEM image of peptide **6** does not show any kind of fibrillar morphology in the solid state.

The morphological resemblance of peptide **1**, **2** and **3** fibrils with amyloid plaque was also studied by Congo red staining. It has been reported that Congo red binds with amyloid fibrils responsible for various neurodegenerative diseases like Alzheimer's disease, Parkinson's disease and shows distinct birefringence under polarized light.[17] To determine the similarity of these aggregated fibrils with Alzheimer's β-amyloid fibrils, fibrils obtained from peptides **1**, **2** and **3** have been stained with Congo red and observed through cross polarizers. All these peptide fibrils bind with Congo red and exhibit typical birefringence under a polarized microscope. Fig. 9(a) shows a typical green-gold birefringence of Congo red bound fibrils of peptide **2** viewed through a cross polarizer. These results are consistent with Congo red binding to an amyloid cross-β-sheet fibrillar structure.[18] Peptides **4**, **5** and **6** do not exhibit typical birefringence when they are stained with Congo red and viewed through cross polarizers. Fig. 9(b) does not show any birefringence when peptide **5** is stained with Congo red and viewed under a polarized microscope.

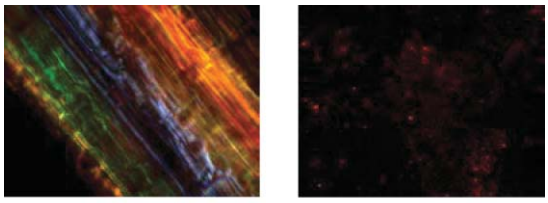

(a) (b)

Fig. 9 Optical microscopic images of (a) peptide **2** fibrils stained with a Congo red dye showing a green-gold birefringence, a characteristic feature of amyloid fibrils and (b) peptide **5** stained with a Congo red dye does not show any birefringence observed at 100 × magnification between crossed polarizers.

From the FT-IR studies of peptides **1–6**, it is clear that all these peptides form intermolecularly hydrogen-bonded sheet-like aggregated structures. The single crystal X-ray structure of peptide **1** clearly established that it has self-assembled to form an intermolecularly hydrogen-bonded supramolecular β-sheet structure and it forms amyloid-like fibrils in the solid state upon further aggregation. Similar fibrillation has been observed for peptides **2** and **3** containing disulfide bonds. All these peptide fibrils bind with a physiological Congo red dye and exhibit typical birefringence under a cross polarizer suggesting the similarity of these fibrils to amyloid fibrils. However, peptides in which disulfide bonds are reduced (peptides **4**, **5** and **6**) are unable to form any kind of fibrillation. This clearly indicates that disulfide bonds must play a definite role in amyloid-like fibril formation in our model peptide system. It has also been reported that the disulfide linkage plays a crucial role in amyloid fibril formation from various non-related amyloidogenic proteins.[10–12] The linkage between the disulfide bond and fibril formation is closely related. Our model peptide system vividly demonstrates the role of the disulfide bridge in the formation of amyloid-like fibrils.

Conclusions

This paper clearly demonstrates that peptide **1** containing a disulfide bond self-assembles to form an intermolecularly hydrogen-bonded antiparallel supramolecular β-sheet structure, as it is apparent from its single crystal X-ray diffraction study. The subunit of the supramolecular β-sheet of peptide **1** is a new motif, a non-intramolecularly hydrogen bonded structure with a buried interchain disulfide bond. This peptide and other structurally related peptides **2** and **3** form fibrils upon further aggregation. FT-IR data indicate that these other peptides (**2** and **3**) containing disulfide bonds also form intermolecularly hydrogen-bonded β-sheet like structures. These fibrils show a close resemblance to amyloid fibrils. However, peptides **4**, **5** and **6** without any disulfide bonds have failed to form amyloid-like fibrils under the same conditions. This establishes the role of the disulfide bond in amyloid-like fibril formation in our model peptide studies. So, this study of amyloid-like fibril forming

model peptides with antiparallel β-sheet structures containing a disulfide bond at atomic resolution, may assist in understanding the self-assembly mechanism of amyloid fibril formation and the role of the disulfide bond in this type of fibrillation. It is an important issue to find out the specific cause for the loss of fibril formation after reducing the disulfide bridge. It might be the increased molecular weight (*i. e.* the larger hydrogen bonding capacity per unit) and/or the presence of the disulfide bond itself. Studies regarding this direction are yet to be explored and it is going on in our laboratory.

Experimental

Synthesis of peptides

The dipeptide subunits **1**, **2** and **3** employed in this report were synthesized by conventional solution phase methodology.[19] The Boc group was used for N-terminal protection and the C-terminus was protected as a methyl ester. Couplings were mediated by dicyclohexylcarbodiimide–1-hydroxybenzotriazole (DCC–HOBt). The final compounds were fully characterized by IR spectroscopy, ^{1}H NMR spectroscopy and mass spectrometry.

Bis[Boc–D-Leu(1)–Cys(2)–OMe] 1

Boc–D-Leu(1)–OH 7. A solution of D-leucine (1.31 g, 10 mmol) in a mixture of dioxan (20 mL), water (10 mL) and 1 M NaOH (10 mL) was stirred and cooled in an ice–water bath. Di-*tert*-butylpyrocarbonate (2.4 g, 11 mmol) was added and stirring was continued at room temperature for 6 h. Then the solution was concentrated *in vacuo* to about 40–60 mL, cooled in an ice–water bath, covered with a layer of ethyl acetate (about 50 mL) and acidified with a dilute solution of $KHSO_4$ to pH 2–3 (Congo red). The aqueous phase was extracted with ethyl acetate and this operation was done repeatedly. The ethyl acetate extracts were pooled, washed with water and dried over anhydrous Na_2SO_4 and evaporated *in vacuo*. Pure material was obtained as a white solid.

Yield = 2.01 g (8.7 mmol, 87%).

Bis[Boc–D-Leu(1)–Cys(2)–OMe] 1. 1.96 g (8.5 mmol) of Boc–D-Leu(1)–OH **7** in 15 mL of DMF were cooled in an ice–water bath and H–cystine–OMe was isolated from 2.9 g (8.5 mmol) of the corresponding methyl ester hydrochloride by neutralization and subsequent extraction with ethyl acetate and the ethyl acetate extract was concentrated to 8 mL. It was then added to the reaction mixture, followed immediately by 1.75 g (8.5 mmol) DCC and 1.15 g (8.5 mmol) of HOBt. The reaction mixture was stirred for three days. The residue was taken up in ethyl acetate (40 mL) and the DCU was filtered off. The organic layer was washed with 2 M HCl (3 × 40 mL), brine (2 × 50 mL), 1 M sodium carbonate (3 × 40 mL), brine (2 × 40 mL), dried over anhydrous sodium sulfate and evaporated *in vacuo* to yield **1** as a white solid. Purification was done by silica gel column (100–200 mesh) using chloroform–methanol as eluent. Yield = 2.5 g (3.6 mmol, 84.7%). (Found: C, 51.89; H, 7.82; N, 8.1%. $C_{30}H_{54}N_4O_{10}S_2$ requires: C, 51.87; H, 7.78; N, 8.07%); IR(KBr): 3331, 1730, 1692, 1655, 1532 cm^{-1}; $[a]_D^{20}$ = +74.7 (*c* 0.2, $CHCl_3$); ^{1}H NMR (300 MHz, $CDCl_3$) δ 7.09 (Cys(2) NH, 2H, d, J = 9 Hz), 4.99 (D-Leu(1) NH, 2H, d, J = 11.2 Hz), 4.79 (C^{α}H of Cys(2), 2H, m), 4.19 (C^{α}H of D-Leu(1), 2H, m), 3.76 (–OCH_3, 6H, s), 3.19 (C^{β}Hs Cys(2), 4H, m), 1.66 (C^{β}Hs & C^{γ}H of D-Leu(1), 6H, m), 1.45 (Boc–CH_3s, 18H, s), 0.92 (C^{δ}Hs of D-Leu(1), 12H, m). ESI–MS $(M + Na)^+$ = 717.2, M_{calcd} = 694.

Bis[Boc–Leu(1)–Cys(2)–OMe] 2

Boc–Leu(1)–OH 8. See ref. 20.

Bis[Boc–Leu(1)–Cys(2)–OMe] 2. 1.96 g (8.5 mmol) of Boc–Leu(1)–OH **8** in 15 mL of DMF were cooled in an ice–water bath and H–cystine–OMe was isolated from 2.9 g (8.5 mmol) of the corresponding methyl ester hydrochloride by neutralization and subsequent extraction with ethyl acetate and the ethyl acetate extract was concentrated to 8 mL. It was then added to the reaction mixture, followed immediately by 1.75 g (8.5 mmol) DCC and 1.15 g (8.5 mmol) of HOBt. The reaction mixture was stirred for three days. The residue was taken up in ethyl acetate (40 mL) and the DCU was filtered off. The organic layer was washed with 2 M HCl (3 × 40 mL), brine (2 × 50 mL), 1 M sodium carbonate (3 × 40 mL), brine (2 × 40 mL), dried over anhydrous sodium sulfate and evaporated *in vacuo* to yield **2** as a white solid. Purification was done by silica gel column (100–200 mesh) using chloroform–methanol as eluent. Yield = 2.57 g (3.7 mmol, 87.1%). (Found: C, 51.85; H, 7.68; N, 8.11%. $C_{30}H_{54}N_4O_{10}S_2$ requires: C, 51.87; H, 7.78; N, 8.07%); IR(KBr): 3315, 1749, 1664, 1540 cm^{-1}; $[a]_D^{20}$ = +47.4 (*c* 0.21, $CHCl_3$); ^{1}H NMR (300 MHz, $CDCl_3$) δ 7.6 (Cys(2) NH, 2H, d, J = 6.8 Hz), 5.24 (Leu(1) NH, 2H, d, J = 8.3 Hz), 4.89 (C^{α}H of Cys(2), 2H, m), 4.30 (C^{α}H of Leu(1), 2H, m), 3.75 (–OCH_3, 6H, s), 3.12 (C^{β}Hs Cys(2), 4H, m), 1.65 (C^{β}Hs & C^{γ}H of Leu(1), 6H, m), 1.43 (Boc–CH_3s, 18H, s), 0.93 (C^{δ}Hs of Leu(1), 12H, m). MALDI-MASS $(M + Na)^+$ = 717.1, M_{calcd} = 694.

Bis[Boc–Val(1)–Cys(2)–OMe] 3

Boc–Val(1)–OH 9. A solution of valine (1.17 g, 10 mmol) in a mixture of dioxan (20 mL), water (10 mL) and 1 M NaOH (10 mL) was stirred and cooled in an ice–water bath. Di-*tert*-butylpyrocarbonate (2.4 g, 11 mmol) was added and stirring was continued at room temperature for 6 h. Then the solution was concentrated *in vacuo* to about 40–60 mL, cooled in an ice–water bath, covered with a layer of ethyl acetate (about 50 mL) and acidified with a dilute solution of $KHSO_4$ to pH 2–3 (Congo red). The aqueous phase was extracted with ethyl acetate and this operation was done repeatedly. The ethyl acetate extracts were pooled, washed with water and dried over anhydrous Na_2SO_4 and evaporated *in vacuo*. Pure material was obtained as a white solid. Yield = 1.91 g (8.8 mmol, 88%).

Bis[Boc–Val(1)–Cys(2)–OMe] 3. 1.84 g (8.5 mmol) of Boc–Val(1)–OH **9** in 15 mL of DMF were cooled in an ice–water bath and H–cystine–OMe was isolated from 2.9 g (8.5 mmol) of the corresponding methyl ester hydrochloride by neutralization and subsequent extraction with ethyl acetate and the ethyl acetate extract was concentrated to 8 mL. It was then added to the reaction mixture, followed immediately by 1.75 g (8.5 mmol) DCC and 1.15 g (8.5 mmol) of HOBt. The reaction mixture was stirred for three days. The residue was taken up in ethyl acetate (40 mL) and the DCU was filtered off. The organic layer was washed with 2 M HCl (3 × 40 mL), brine (2 × 50 mL), 1 M sodium carbonate (3 × 40 mL), brine (2 × 40 mL), dried over anhydrous sodium sulfate and evaporated *in vacuo* to yield **3** as a white solid. Purification was done by silica gel column (100–200 mesh) using chloroform–methanol as eluent. Yield = 2.4 g (3.6 mmol, 85%). (Found: C, 50.49; H, 7.49; N, 8.35%. $C_{28}H_{50}N_4O_{10}S_2$ requires: C, 50.45; H, 7.51; N, 8.41%); IR(KBr): 3330, 1748, 1691, 1654, 1532 cm^{-1}; $[a]_D^{20}$ = +69.9 (*c* 0.21, $CHCl_3$); ^{1}H NMR (300 MHz, $CDCl_3$) δ 7.46 (Cys(2) NH, 2H, d, J = 6.6 Hz), 5.36 (Val(1) NH, 2H, d, J = 8.6 Hz), 4.91 (C^{α}H of Cys(2), 2H, m), 4.08–4.13 (C^{α}H of Val(1), 2H, m), 3.75 (OCH_3, 6H, s), 3.09 (C^{β}Hs Cys(2), 4H, m), 2.07 (C^{β}H of Val(1), 2H, m), 1.43 (Boc–CH_3s, 18H, s), 0.99 (C^{γ}Hs of Val(1), 12H, m). ESI-MS $(M + Na)^+$ = 689.3, M_{calcd} = 666.

The disulfide bonds of peptides **1**, **2** and **3** were reduced by refluxing with indium and NH_4Cl at 60 °C in dry ethanol for 2 hours to obtain the peptides Boc–D-Leu(1)–Cys(2)–OMe **4**, Boc–Leu(1)–Cys(2)–OMe **5** and Boc–Val(1)–Cys(2)–OMe **6**.[21]

Boc–D-Leu(1)–Cys(2)–OMe 4. (Found: C, 51.75; H, 8.07; N, 8.1%. $C_{15}H_{28}N_2O_5S$ requires: C, 51.72; H, 8.05; N, 8.05%); IR(KBr): 3341, 2383, 1751, 1686, 1662, 1527 cm^{-1}; $[a]_D^{20}$ = +70.5 (*c* 1.12, $CHCl_3$); ^{1}H NMR (300 MHz, $CDCl_3$) δ 7.10 (Cys(2) NH,

1H, d, $J = 6$ Hz), 5.00 (D-Leu(1) NH, 1H, d, $J = 9$ Hz), 4.78 ($C^{\alpha}H$ of Cys(2), 1H, m), 4.18 ($C^{\alpha}H$ of D-Leu(1), 1H, m), 3.78 (OCH_3, 3H, s), 3.19 ($C^{\beta}Hs$ Cys(2), 2H, m), 1.64 ($C^{\beta}Hs$ & $C^{\gamma}H$ of D-Leu(1), 3H, m), 1.45 (Boc–CH_3s, 9H, s), 0.94 ($C^{\delta}Hs$ of D-Leu(1), 6H, m). ESI-MS $(M + Na)^+ = 371.2$, $M_{calcd} = 348$.

Boc–Leu(1)–Cys(2)–OMe 5. (Found: C, 51.7; H, 8.02; N, 8.09%. $C_{15}H_{28}N_2O_5S$ requires: C, 51.72; H, 8.05; N, 8.05%); IR(KBr): 3337, 2566, 1715, 1679, 1540 cm^{-1}; $[a]_D^{20} = +23.8$ (c 1.1, $CHCl_3$); ^1H NMR (300 MHz, $CDCl_3$) δ 7.63 (Cys(2) NH, 1H, d, $J = 6.3$ Hz), 5.31 (Leu(1) NH, 1H, d, $J = 7.8$ Hz), 4.86 ($C^{\alpha}H$ of Cys(2), 1H, m), 4.30 ($C^{\alpha}H$ of Leu(1), 1H, m), 3.74 (OCH_3, 3H, s), 3.08 ($C^{\beta}Hs$ Cys(2), 2H, m), 1.68 ($C^{\beta}Hs$ & $C^{\gamma}H$ of Leu(1), 3H, m), 1.42 (Boc-CH_3s, 9H, s), 0.93 ($C^{\delta}Hs$ of Leu(1), 6H, m). ESI-MS $(M + Na)^+ = 371.4$, $M_{calcd} = 348$.

Boc–Val(1)–Cys(2)–OMe 6. (Found: C, 50.35; H, 7.75; N, 8.43%. $C_{14}H_{26}N_2O_5S$ requires: C, 50.3; H, 7.78; N, 8.38%); IR(KBr): 3330, 2354, 1747, 1689, 1653, 1531 cm^{-1}; $[a]_D^{20} = +49.4$ (c 1.02, $CHCl_3$); ^1H NMR (300 MHz, $CDCl_3$) δ 7.45 (Cys(2) NH, 1H, d, $J = 5.7$ Hz), 5.37 (Val(1) NH, 1H, d, $J = 8.6$ Hz), 4.90 ($C^{\alpha}H$ of Cys(2), 1H, m), 4.13 ($C^{\alpha}H$ of Val(1), 1H, m), 3.75 (OCH_3, 3H, s), 3.11 ($C^{\beta}Hs$ Cys(2), 2H, m), 2.11 ($C^{\beta}H$ of Val(1), 1H, m), 1.43 (Boc–CH_3s, 9H, s), 0.96 ($C^{\gamma}Hs$ of Val(1), 6H, m). ESI-MS $(M + Na)^+ = 357.4$, $M_{calcd} = 334$.

NMR experiments

All NMR studies were carried out on a Brucker DPX 300 MHz spectrometer at 300 K. Peptide concentrations were in the range 1–10 mM in $CDCl_3$.

FT-IR spectroscopy

The FT-IR spectra were taken using a Shimadzu (Japan) model FT-IR spectrophotometer. The solid-state FT-IR measurements were performed using the KBr disk technique.

Scanning electron microscopic study

Morphologies of all reported tripeptides were investigated using scanning electron microscopy (SEM). For the SEM study, fibrous materials (slowly grown from methanol–water mixtures) were dried and gold coated. Then the micrographs were taken in a SEM apparatus (Jeol Scanning Microscope—JSM-5200 and Jeol Scanning Microscope—JSM-6700F).

Transmission electron microscopic study

The morphologies of the reported compounds were investigated using transmission electron microscopy (TEM). Transmission electron microscopic studies of peptide **1** were carried out using a small amount of the solution of the corresponding compound on carbon-coated copper grid (200 mesh) by slow evaporation and vacuum drying at 30 °C for two days. Images were taken at an accelerating voltage of 200 kV. TEM was performed using a JEM-2010 electron microscope.

Congo red binding study

An alkaline saturated Congo red solution was prepared. The peptide fibrils were stained by alkaline Congo red solution (80% methanol–20% glass distilled water containing 10 mL of 1% NaOH) for 2 min and then the excess stain (Congo red) was removed by rinsing the stained fibril with 80% methanol–20% glass distilled water solution several times. The stained fibrils were dried under vacuum at room temperature for 24 h, then visualized at 100 × magnification and birefringence was observed between crossed polarizers.

Crystal data for peptide 1

$C_{30}H_{54}N_4O_{10}S_2$, Mw = 694.91, monoclinic, space group $C2$, $a = 25.41(3)$, $b = 5.071(7)$, $c = 15.318(17)$ Å, $\beta = 106.77(10)°$, $U = 1890$ Å^3, $Z = 2$, $D_{calc} = 1.221$ g cm^{-3}. Intensity data were collected with MoKα radiation using the MARresearch Image Plate System. The crystal was positioned at 70 mm from the Image Plate. 100 frames were measured at 2° intervals with a counting time of 5 min to give 2802 independent reflections. Data analysis was carried out with the XDS program.[22] The structure was solved using direct methods with the Shelx86 program.[23] The non-hydrogen atoms were refined with anisotropic thermal parameters. The hydrogen atoms were included in geometric positions and given thermal parameters equivalent to 1.2 times those of the atom to which they were attached. The structure was refined on F^2 using Shelxl.[24] The final R values were $R1$ 0.0807 and $wR2$ 0.1785 for 2488 data with $I > 2\sigma(I)$. The largest peak and hole in the final difference Fourier were 0.43 and −0.26 e Å^{-3}.†

Acknowledgements

We thank the EPSRC and the University of Reading, UK for funds for the Image Plate System. This research was also supported by a grant from the Department of Science and Technology (DST), India (project no. SR/S5/OC-29/2003). A. K. Das wishes to acknowledge the CSIR, New Delhi, India for financial assistance.

References

1 C. E. MacPhee and D. N. Woolfson, *Curr. Opin. Solid State Mater. Sci.*, 2004, **8**, 141–149; W. Wang and M. H. Hecht, *Proc. Natl. Acad. Sci. USA*, 2002, **99**, 2760–2765; D. E. Otzen, O. Kristensen and M. Oliveberg, *Proc. Natl. Acad. Sci. USA*, 2000, **97**, 9907–9912; M. T. Krejchi, E. D. T. Atkins, A. J. Waddon, M. J. Fournier, T. L. Mason and D. A. Tirrell, *Science*, 1994, **265**, 1427–1432.

2 G. von Maltzahn, S. Vauthey, S. Santoso and S. Zhang, *Langmuir*, 2003, **19**, 4332–4337; D. T. Bong, T. D. Clark, J. R. Granja and M. R. Ghadiri, *Angew. Chem., Int. Ed.*, 2001, **40**, 988–1011; J. M. Lehn, *Science*, 1993, **260**, 1762–1763; G. M. Whitesides, J. P. Mathias and C. T. Seto, *Science*, 1991, **254**, 1312–1319.

3 T. C. Holmes, S. D. Lacalle, X. Su, G. Liu, A. Rich and S. Zhang, *Proc. Natl. Acad. Sci. USA*, 2000, **97**, 6728–6733.

4 R. Baumeister and S. Eimer, *Angew. Chem., Int. Ed.*, 1998, **37**, 2978–2982; P. T. Lansbury, Jr., *Acc. Chem. Res.*, 1996, **29**, 317–321; J. C. Rochet and P. T. Lansbury, Jr., *Curr. Opin. Struct. Biol.*, 2000, **10**, 60–68; D. M. Walsh, A. Lomakin, G. B. Benedek, M. M. Condron and D. B. Teplow, *J. Biol. Chem.*, 1997, **272**, 22364–22372; M. F. Perutz, J. T. Finch, J. Berriman and A. Lesk, *Proc. Natl. Acad. Sci. USA*, 2002, **99**, 5591–5595; G. Taubes, *Science*, 1996, **271**, 1493–1495; S. L. Bernstein, T. Wyttenbach, A. Baumketner, J.-E. Shea, G. Bitan, D. B. Teplow and M. T. Bowers, *J. Am. Chem. Soc.*, 2005, **127**, 2075–2084.

5 M. F. Perutz, *Curr. Opin. Struct. Biol.*, 1996, **6**, 848–858; M. E. MacDonald and J. F. Gusella, *Curr. Opin. Neurobiol.*, 1996, **6**, 638–643.

6 M. Goedert, M. G. Spillntini and S. W. Davies, *Curr. Opin. Neurobiol.*, 1998, **8**, 619–632; M. G. Spillantini, R. A. Crowther, R. Jakes, M. Hasegawa and M. Goedert, *Proc. Natl. Acad. Sci. USA*, 1998, **95**, 6469–6473.

7 S. B. Prusiner, *Proc. Natl. Acad. Sci. USA*, 1998, **95**, 13363–13383; M. A. Baldwin, F. E. Cohen and S. B. Prusiner, *J. Biol. Chem.*, 1995, **270**, 19197–19200; S. B. L. Ng and A. J. Doig, *Chem. Soc. Rev.*, 1997, **26**, 425–432.

8 R. Azriel and E. Gazit, *J. Biol. Chem.*, 2001, **276**, 34156–34161; J. D. Sipe and A. S. Cohen, *J. Struct. Biol.*, 2000, **130**, 88–98; Y. Porat, S. Kolusheva, R. Jelinek and E. Gazit, *Biochemistry*, 2003, **42**, 10971–10977.

9 A. Sanbe, H. Osinska, J. E. Saffitz, C. G. Glabe, R. Kayed, A. Maloyan and J. Robbins, *Proc. Natl. Acad. Sci. USA*, 2004, **101**, 10132–10136; J. H. Magnus, T. Stenstad, S. O. Kolset and G. Husby, *Scand. J. Immunol.*, 2001, **34**, 63–69.

10 Y. Ohhashi, Y. Hagihara, G. Kozhukh, M. Hoshino, K. Hasegawa, I. Yamaguchi, H. Naiki and Y. Goto, *J. Biochem.*, 2002, **131**, 45–52; D.-P. Hong, M. Gozu, K. Hasegawa, H. Naiki and Y. Goto, *J. Biol. Chem.*, 2002, **277**, 21554–21560.

11 Q. Zhang and J. W. Kelly, *Biochemistry*, 2003, **42**, 8756–8761.

12 O. M. A. El-Agnaf, J. M. Sheridan, C. Sidera, G. Siligardi, R. Hussain, P. I. Haris and B. M. Austen, *Biochemistry*, 2001, **40**, 3449–3457.

† CCDC reference number 276179. See http://dx.doi.org/10.1039/b509083k for crystallographic data in CIF or other electronic format.

13 R. P. Lyon and W. M. Atkins, *J. Am. Chem. Soc.*, 2001, **123**, 4408–4413.
14 S. K. Maji, M. G. B. Drew and A. Banerjee, *Chem. Commun.*, 2001, **123**, 1946–1947; A. Banerjee, S. K. Maji, M. G. B. Drew, D. Haldar and A. Banerjee, *Tetrahedron Lett.*, 2003, **44**, 6741–6744; A. Banerjee, S. K. Maji, M. G. B. Drew, D. Haldar and A. Banerjee, *Tetrahedron Lett.*, 2003, **44**, 335–339; S. K. Maji, D. Haldar, M. G. B. Drew, A. Banerjee, A. K. Das and A. Banerjee, *Tetrahedron*, 2004, **60**, 3251–3259; A. Banerjee, S. K. Maji, M. G. B. Drew, D. Haldar, A. K. Das and A. Banerjee, *Tetrahedron*, 2004, **60**, 5935–5944.
15 G. N. Ramachandran and V. Sasisekharan, *Adv. Protein Chem.*, 1968, **23**, 284–438.
16 G. P. Dado and S. H. Gellman, *J. Am. Chem. Soc.*, 1994, **116**, 1054–1062; V. Moretto, M. Crisma, G. M. Bonora, C. Toniolo, H. Balaram and P. Balaram, *Macromolecules*, 1989, **22**, 2939–2944.
17 M. L. dela-Paz and L. Serrano, *Proc. Natl. Acad. Sci. USA*, 2004, **101**, 87–92; R. A. Krammer, D. Kostrewa, J. Zurdo, A. Detken, C. Garcia-Echeverria, J. D. Green, S. A. Müller, B. H. Meier, F. K. Winkler, C. M. Dobson and M. O. Steinmetz, *Proc. Natl. Acad. Sci. USA*, 2004, **101**, 4435–4440; A. Fernandez, J. Kardos, L. R. Scott, Y. Goto and R. S. Berry, *Proc. Natl. Acad. Sci. USA*, 2003, **100**, 6446–6451.
18 Y. S. Kim, T. W. Randolph, M. C. Manning, F. J. Stevens and J. F. Carpenter, *J. Biol. Chem.*, 2003, **278**, 10842–10850; D. L. Taylor, R. D. Allen and E. P. Benditt, *J. Histochem. Cytochem.*, 1974, **22**, 1105–1112; A. Lim, A. M. Makhov, J. Bond, H. Tnouye, L. H. Conmors, J. D. Griffith, W. B. Erickson, D. A. Kirschner and C. E. Costello, *J. Struct. Biol.*, 2000, **130**, 363–370.
19 M. Bodanszky and A. Bodanszky, *The Practice of Peptide Synthesis*, Springer-Verlag, New York, 1984, pp. 1–282.
20 I. L. Karle, A. Banerjee, S. Bhattacharjya and P. Balaram, *Biopolymers*, 1996, **38**, 515–526.
21 G. V. S. Reddy, G. V. Rao and D. S. Iyengar, *Synth. Commun.*, 2000, **30**, 859–862.
22 W. Kabsh, *J. Appl. Crystallogr.*, 1988, **21**, 916–932.
23 G. M. Sheldrick, *Acta Crystallogr., Sect. A: Fundam. Crystallogr.*, 1990, **46**, 467–480.
24 G. M. Sheldrick, *Program for Crystal Structure Refinement*, University of Göttingen, Germany, 1993.